



ELSEVIER

Available online at www.sciencedirect.com

SCIENCE @ DIRECT®

Journal of Magnetism and Magnetic Materials 266 (2003) 79–87

M Journal of
M magnetism
M and
magnetic
materials

www.elsevier.com/locate/jmmm

Combined reactions associated with $L1_0$ ordering

T.J. Klemmer^{a,*}, C. Liu^a, N. Shukla^a, X.W. Wu^a, D. Weller^a, M. Tanase^b,
D.E. Laughlin^b, W.A. Soffa^c

^aSeagate Research, 1251 Waterfront Place, Pittsburgh, PA 15222, USA

^bData Storage Systems Center, Carnegie Mellon University, Pittsburgh, PA 15261, USA

^cDepartment of Materials Science and Engineering, University of Pittsburgh, Pittsburgh, PA 15213, USA

Received 23 October 2002

Abstract

Recently, self-organized magnetic arrays (SOMAs) have received a great deal of attention because of the potential of achieving magnetic data storage densities greater than 1 Tbit/in². SOMA involves the chemical preparation of self-assembled arrays of alloyed nanoparticles (such as FePt), which can be subsequently annealed to form an $L1_0$ high magnetocrystalline anisotropy chemically ordered phase. However, during the anneal of the nanoparticles the system can further lower its energy by the elimination of surface area which is brought about by another solid-state reaction which is sintering. Therefore, the combined reactions of ordering and sintering must be understood in a systematic way. Previous work on $L1_0$ bulk alloys are reviewed with particular emphasis on the role of combined reactions such as ordering and recrystallization. A methodology is described to help in the understanding of combined reactions involving ordering and solid-state reactions concerning the elimination of crystalline defects such as dislocations, grain boundaries and external surfaces. As a first attempt, this framework based on bulk solid-state reactions is developed and further discussed for the case of SOMA nanoparticles.

© 2003 Elsevier B.V. All rights reserved.

Keywords: Chemical ordering; $L1_0$; Nanoparticles; Recrystallization; Combined reaction; Sintering

1. Introduction

Chemically ordered $L1_0$ alloys such as FePt, CoPt, FePd and MnAl are of interest for permanent magnet applications because of their high magnetocrystalline anisotropy of $\sim 10^7$ – 10^8 ergs/cm³ which is intrinsic to the tetragonal symmetry of the crystal structure. These applications range from bulk permanent magnets [1] to

future, thermally stable high-density magnetic recording media [2]. Recently, self-organized magnetic array (SOMA) media based on $L1_0$ formation in monodispersed nanoparticles has been established as having the potential to be able to postpone the superparamagnetic limit to recording densities [3] beyond 1 Tbit/in². Through a deposition method, these nanoparticles are assembled on a regular two-dimensional (2-D) lattice shown in Fig. 1, which gives the possibility of using them as patterned media. Typically, the material synthesis route of these permanent magnet alloys involves the production of a

*Corresponding author.

E-mail address: timothy.j.klemmer@seagate.com
(T.J. Klemmer).

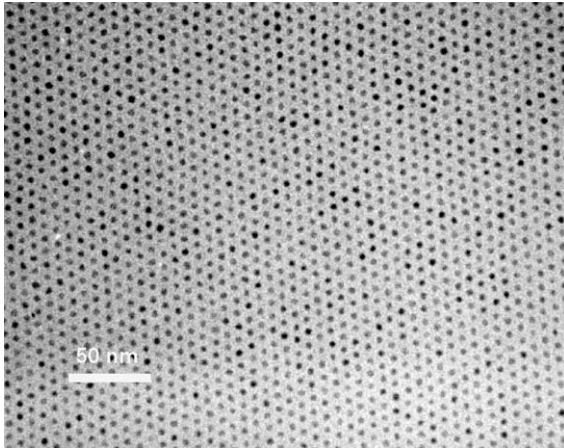


Fig. 1. SOMA of as-deposited FePt nanoparticles.

quenched-in, low anisotropy disordered FCC phase (A1) and annealing in the 500–700°C regime is needed to produce the desired high anisotropy chemically ordered L1₀ phase. However, annealing at such temperatures also typically leads to grain growth and sintering or coalescence [4], which for the case of SOMA media destroys the regular microstructure and therefore poses a serious limitation on the performance of such media. An example of this sintering problem is shown in Fig. 2. Clearly, the advantages of small size, mono-dispersed size and a 2-D lattice of SOMA have been lost. In order to eventually realize the potential of SOMA, these detrimental effects must be avoided while still allowing for the phase transformation of L1₀ ordering. Therefore, it is critical to understand the ordering transformation when it has the possibility of occurring with other solid-state reactions. An attempt is made to understand the chemical ordering transformation in the framework of bulk solid-state reactions.

The chemical ordering of bulk L1₀ alloys such as FePt, CoPt and FePd has been studied in great detail and is known to be similar to the ordering in the prototypical CuAu alloy. However, when the pre-annealed state involves a high density of crystalline defects such as dislocations, grain boundaries and/or surfaces, additional, well-known solid-state reactions such as recrystallization, grain growth and sintering can occur simultaneously with the thermodynamically driven

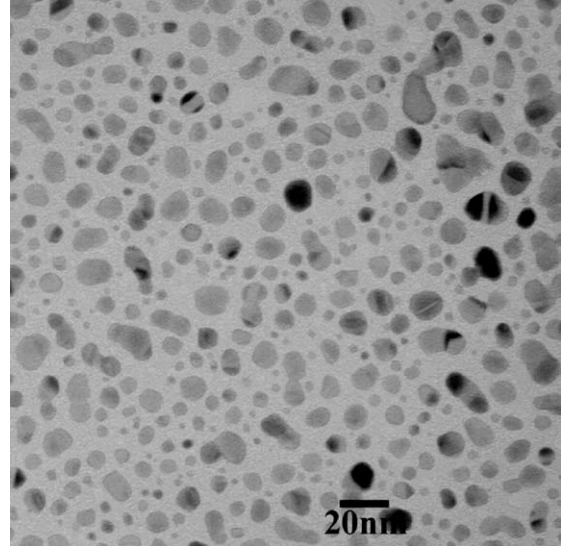


Fig. 2. SOMA after a high temperature anneal used to produce the highly anisotropic L1₀ phase.

ordering transformation. Hornbogen [5] has previously put forth a systematic way of looking at the combined reactions of solid-state transformations involving a change in crystal structure, a change in composition, the annealing out of defects or the crystallization of amorphous alloys. In Hornbogen's original treatment, the chemical ordering of L1₀ alloys was not discussed directly. In this paper, the chemical ordering of L1₀ alloys is discussed and particular emphasis is placed on the effects of annealing on the microstructure when the pre-annealed state involves a highly defective atomically disordered crystalline structure.

2. Kinetics and driving force for ordering

The driving force per unit volume for the FCC (A1) to L1₀ transformation can be estimated from

$$\Delta G_v = \frac{\Delta H_v \Delta T}{T_{\text{crit}}},$$

where ΔH_v is the enthalpy of ordering and ΔT is the undercooling below the critical temperature ($T_{\text{crit}} = T_c$) for ordering [6]. A rough estimate of the configurational enthalpy for the equiatomic FCC to L1₀ ordering reaction can be calculated

using the quasi-chemical approach of Guggenheim [7] to be $\Delta H_v = -0.314RT_{\text{crit}}$, where R is the gas constant. Using this approach for FePt, CoPt and FePd annealed at $\sim 425^\circ\text{C}$, 525°C and 600°C the driving force for $L1_0$ ordering can be calculated and is shown in Table 1. According to the Landau–Lifshitz [8] symmetry rules the A1 to $L1_0$ ordering reaction must be a first-order transformation. This means that ordering usually proceeds by a nucleation and growth process, where an interphase interface is created between ordered and disordered regions. However, at very large undercoolings (below the instability temperature) it is possible for the system to order continuously (spinodal ordering) without a nucleation step [9].

Fig. 3a displays a schematic of a time–temperature–transformation (TTT) diagram for the $L1_0$ ordering reaction, which shows the time it takes for a certain fraction of the total volume to be transformed for different temperatures. Because of the variation of the driving force with undercooling and decreasing atomic mobility at low temperature the ordering reaction is known to exhibit so-called ‘C-curve’ kinetics. This C-curve kinetics have been measured for the $L1_0$ ordering in a bulk FePd alloy [10]. The onset of the nucleation process can be shown theoretically to follow

Table 1
Driving forces for selected solid-state transformations

Solid-state reaction	Driving force (J/m ³)
Recrystallization	10^6 – 10^7
Sintering	1×10^9
Grain growth	2.5×10^8
Ordering (FePd)	6×10^6 at 600°C 3×10^7 at 525°C 6×10^7 at 425°C
Ordering (FePt)	2.5×10^8 at 600°C 3×10^8 at 525°C 3.4×10^8 at 425°C
Ordering (CoPt)	6.9×10^7 at 600°C 9.3×10^7 at 525°C 1.2×10^8 at 425°C

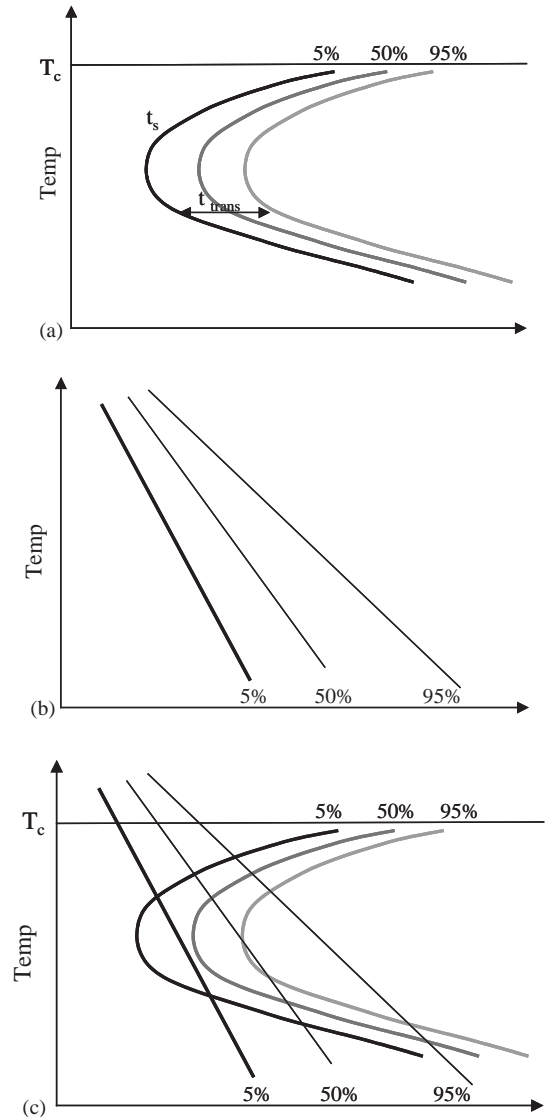


Fig. 3. TTT schematics for (a) $L1_0$ ordering, (b) annealing out of defects and (c) the combined reactions.

$$t_s = t_0 \exp\left(\frac{\Delta G^* + Q_D}{k_B T}\right),$$

where t_0 is a time constant related to the atomic vibrational frequency, Q_D is the activation barrier for diffusion, ΔG^* is the activation barrier for nucleation of the ordered phase and k_B is Boltzmann’s constant [6]. The exact position and shape of the C-curve is related to the specific

mechanism of the ordering transformation and the measured C-curve is given by the mechanism that dominates the transformation. The time it takes for the transformation to proceed from start to finish (t_{trans}) is phenomenologically controlled by the number of transformation fronts (given by the nucleation process) and the growth velocity (v) of the boundary given by

$$v = M \sum_i f_i,$$

where M is the mobility of the interphase interface and f_i are any forces acting on the boundary (driving forces and retarding forces) [5].

3. Conventional $L1_0$ ordering

Most of the past research in these materials focused on the ordering processes of bulk FePt [11,12], CoPt [13] and FePd [11,14], which is similar to the prototypical ordering in CuAu [15] where a disordered FCC phase transforms to the $L1_0$ phase by a coherent nucleation and growth process. An important feature of this transformation is made apparent if we consider the free energy for the formation of an ordered nucleus in a disordered matrix where

$$\Delta G = -V\Delta G_v + A\gamma + V\Delta G_s$$

and V is the volume, A is the surface area and γ is the interfacial energy of ordered nuclei in the disordered matrix. The strain energy (ΔG_s) is associated with the misfit strain resulting from the new ordered particle not fitting perfectly into the space originally occupied by the matrix. Additionally coherency strains at the interface can be present depending on the type of interface. For spherical nuclei, the activation barrier is proportional to $\gamma^3/(\Delta G_v - \Delta G_s)^2$ and the transformation kinetics will select an ordering path, which has a low activation barrier. In bulk, relatively large grained alloys, which are subjected to the FCC to $L1_0$ ordering reaction, the fundamental mechanism involves the precipitation of the ordered phase within the grain. The precipitates form a coherent interface, which has a small γ thereby decreasing the activation energy for

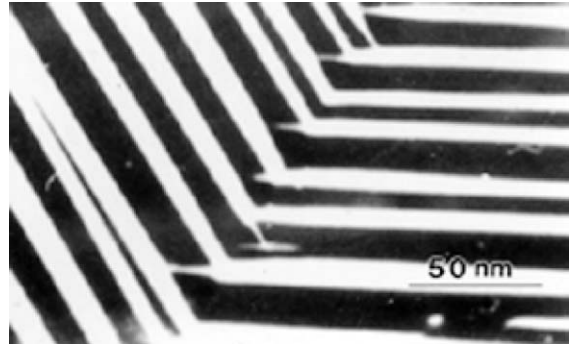


Fig. 4. Typical (101) polytwin structure formed as a result of the $L1_0$ phase transformation in bulk FePd alloys which are not deformed before annealing.

chemical ordering. However, for the A1 to $L1_0$ transformation the strain energy can be appreciable and is caused by the contraction of the c -axis and expansion of the a -axes with respect to the disordered FCC matrix. The strain energy is greatly decreased predominantly by two mechanisms; a metastable state is initially formed with $1 > c/a > (c/a)_{\text{eq}}$ and by the formation of different variants of the c -axis ($c\|(100)_{\text{FCC}}$, $c\|(010)_{\text{FCC}}$ and $c\|(001)_{\text{FCC}}$), which causes an overlapping of the compression and expansion regions surrounding the nuclei. The transformation strain energy can then be further decreased by the stress-induced growth of the ordered phase [16]. The strain energy is relaxed by a long-range reorganization of the nuclei into bands of common variance within the bands and adjacent bands having the c -axis at 90° to the neighboring band. These bands contact each other along a common (101) plane and with subsequent coarsening and growth, a fully ordered structure contains the characteristic microstructure of (101) transformation twins/structural domains shown in Fig. 4 for the case of FePd. As a result of the transformation a large density of antiphase boundaries (APB) is produced which help to pin magnetic domain walls [17].

4. Annealing out of defects

Often materials subjected to the $L1_0$ ordering transformation are driven further from equilibrium

by pre-annealing processing. Examples of such processing are sputtering of thin films [18], melt spinning of ribbons [19], chemical synthesis of nanoparticles [3], ball milling of particles [20] and cold rolling of bulk materials [21]. The additional stored energy is in the form of a high density of crystalline defects (vacancies, dislocations, high-angle grain boundaries and external surfaces) and intrinsic stresses, which when heat-treated will tend to decrease that energy by a variety of different mechanisms such as recovery, recrystallization, grain growth and sintering. As a result, the annealing process concomitant with the ordering process can greatly change the overall transformation into a variety of scenarios. Hornbogen [5] has described the transformation synergistics involved when combined thermomechanical reactions can occur. We will use this approach to discuss the L1₀ ordering transformation of a cold-rolled disordered alloy subjected to annealing.

The driving force for recrystallization can be estimated as

$$\Delta G_v = \alpha \mu b^2 \rho / 2,$$

where μ is the shear modulus, b the Burgers vector, α a constant (~ 0.1 – 1) and ρ the dislocation density [22]. For a highly deformed FCC FePd alloy the driving force can be estimated to be in the range of 10^6 – 10^7 J/m³ [21,23]. It is well known that classical nucleation theory involving thermal fluctuations cannot explain the short times of recrystallization often observed in highly deformed materials. As a result, a theory involving the maturation of nuclei being brought about by a rearrangement of the deformed microstructure via recovery processes has been widely accepted [22]. This theory predicts that the high-angle and high-energy boundaries that act as the reaction front in recrystallization are produced by a condensation of the deformed microstructure.

The driving forces for grain growth and sintering are stored in the amount of interfacial surfaces such as grain boundaries and external surfaces. These driving forces can be estimated as

$$\Delta G_v \propto \frac{\gamma}{r},$$

where for the case of grain growth the γ is the grain boundary energy and r is the grain radius, but for sintering γ is the external surface energy and r is the particle radius. If we assume 2 nm grains or particles, a grain boundary energy [6] $\gamma_{GB} \sim 0.5$ J/m² and a surface energy of $\gamma_{surf} \sim 2$ J/m², we can calculate the driving forces for grain growth and sintering as shown in Table 1.

The driving forces for recrystallization, grain growth and sintering are not temperature dependent since they already exist in the pre-annealed state making these activation barriers essentially temperature independent. As a result the activation barrier can be replaced by one activation barrier Q_m , which is dependent on rearrangement process, the activation barrier for diffusion and the stored energy. The nucleation process still involves an incubation time that is controlled by an activation barrier, which is temperature independent therefore the start of defect driven solid-state transformations will follow

$$t_s = t_0 \exp\left(\frac{Q_m}{k_B T}\right).$$

As a result of the constant driving force with temperature the start for the transformation when plotted on a TTT diagram is a downward sloping line as shown in Fig. 3b whose position on the time axis is controlled by diffusion and rearrangement of the defect structure, which has been described as Q_m .

5. Combined reactions

When looking at schematics for the start of transformation curves of defect driven transformations and chemical ordering together as shown in Fig. 3c it must be realized that their relative positions depend critically on the initial defect state of the material before and during the heat treatment. As a way to simplify the problem, it is helpful to look at the total transformation as two reactions occurring either sequentially or simultaneously. Sequential reactions occur when one solid-state transformation can be driven to completion before the other transformation can start. However, simultaneous reactions occur when the

reactions overlap. In this case it is possible for one reaction to actually help the other reaction and it is possible to substantially shorten the reaction times of one or both transformations.

6. Combined reactions: example of ordering and recrystallization

In the case of bulk FePd which has been heavily cold-rolled before annealing the mechanism of

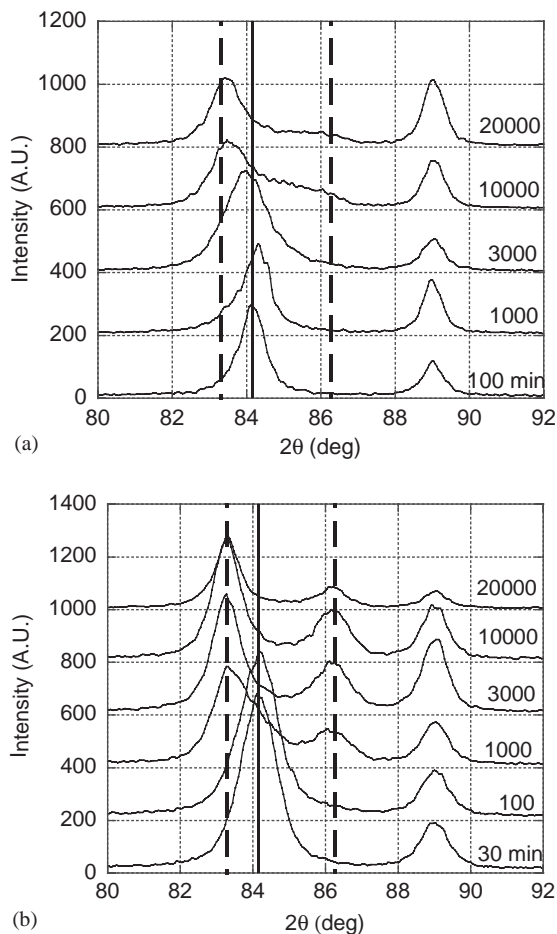


Fig. 5. X-ray diffraction of samples of bulk FePd annealed for different times at 425°C with (a) 0% deformation and (b) 80% deformation. Solid lines mark the position of the (113) peak of the cubic disordered phase while the dotted lines mark the position of the (113) and (311) peaks of the tetragonal $L1_0$ phase.

ordering has been found in certain temperature regimes to change significantly from the mechanism found in the undeformed material [21,23]. Fig. 5a shows XRD spectra for undeformed FePd annealed at 425°C for different amounts of time while Fig. 5b shows the same for highly deformed (cold-rolled ~80%). It is found that the deformation accelerates the ordering process and is observed by the splitting of the (113) peak at a shorter time. The splitting is the result of the disordered cubic FCC structure transforming to the ordered and tetragonal $L1_0$ structure. The 80% deformed sample is found to be essentially completely ordered at ~1000 min, while the undeformed material is still not completely ordered at times of ~20,000 min. This rapid ordering is also observed in the increase of the coercivity with annealing time as shown in Fig. 6 for the two different pre-annealed states.

As stated above it is known that the conventional ordering transformation in large grained bulk $L1_0$ alloys progresses by the motion of a reaction front, which is coherent with the disordered matrix. The observed microstructure after complete transformation is the well-known (101) polytwin structure shown in Fig. 4. Because of the coherent nature of the reaction front, the mobility is relatively sluggish. However, when the as-prepared state is highly deformed the material

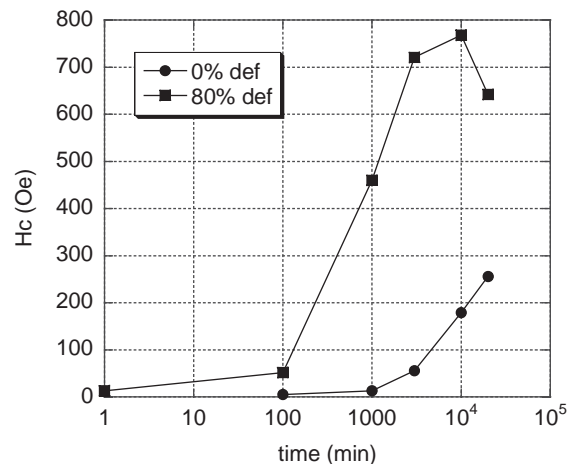


Fig. 6. Coercive field as a function of annealing time at 425°C for 0% deformed and 80% deformed bulk FePd alloys.

can recrystallize by the creation of a high-angle and incoherent boundary, which has a relatively high mobility. As stated above an incubation time is needed for the formation of this new reaction front. An example of this type of boundary is shown in Fig. 7 for the highly deformed FePd alloy. Once the incoherent boundary has formed by the rearrangement of the defect structure, it is possible for the ordered phase to heterogeneously nucleate at this newly developed grain boundary. At this point the combined reactions can occur such that the system lowers its energy (by ordering and the decrease of the defect density) through the migration of the new reaction front, which is the incoherent boundary. This can be visualized by considering the migration of the boundary such that ahead of the boundary is disordered and defective material and in its wake is left ordered material with low defect concentrations. Because of the high mobility and the combined driving forces of the solid-state transformations the velocity of the boundary is greatly enhanced providing a faster mechanism for the ordering process. As a result of the combined reactions the resulting microstructure drastically changes when compared to conventional ordering described above. These new grains contain some defects such as $\{111\}$ nanotwins; however, no $\{101\}$ polytwins are observed. There are also larger $\{111\}$ twins which are presumably formed by the same mechanisms as annealing twins in FCC

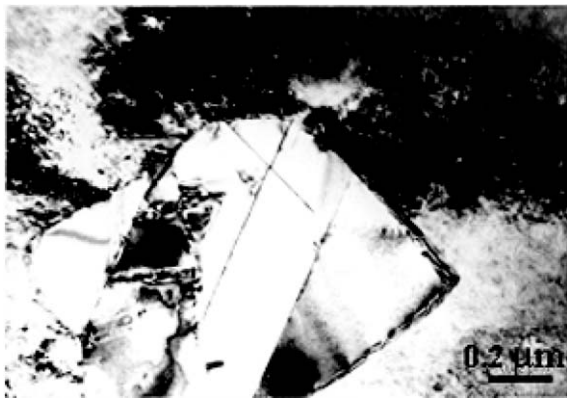


Fig. 7. High-angle transformation front observed in 80% cold-rolled bulk FePd subjected to the combined reactions of ordering and recrystallization.

alloys [24]. The new microstructure is the reason for the enhanced coercivity seen in Fig. 6 for the 80% deformed alloy [23].

7. $L1_0$ ordering in nanoparticulate systems

Recently, SOMA based on FePt $L1_0$ alloys has received a lot of attention based upon their potential for achieving ultra-high-density magnetic recording media. A chemical synthesis is used to produce monodispersed FePt nanoparticles, which are crystalline but are FCC and chemically disordered. An example of the crystallinity and the surface faceting of an as-deposited nanoparticle is shown in Fig. 8. Self-assembly deposition techniques taking advantage of steric repulsive forces from a coating of surfactant on the nanoparticles and natural attractive forces between particles can be used to arrange the nanoparticles on a 2-D lattice making them ideal for patterned media. However, in order to make the nanoparticles thermally stable, annealing is required to transform the nanoparticles into the high magnetocrystalline anisotropic $L1_0$ phase. Because of the small size of the particles (diameter ~ 4 nm) it was shown above that considerable driving forces exist for grain growth and sintering.

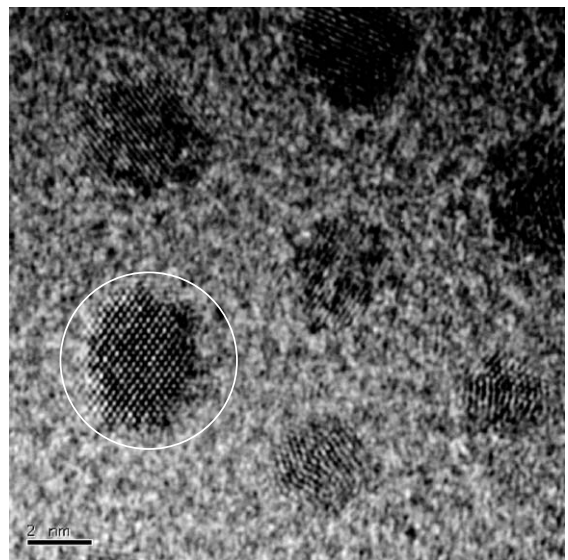


Fig. 8. HRTEM of a lone, as-deposited FePt nanoparticle.

In order to achieve the full potential of SOMA the annealing reaction of the FePt nanoparticles must be controlled and therefore a better understanding of the combined reactions of ordering and the solid-state reactions involving the elimination of interfaces.

Using ideas acquired from the ordering of bulk materials discussed above one can easily make analogies to come up with mechanisms of ordering that should be considered for the ordering of $L1_0$ nanoparticles. One such mechanism is based on the analogy of conventional $L1_0$ ordering and can be described for the ordering of a monocrystalline particle such as in Fig. 8. The nucleation and growth of coherent $L1_0$ nuclei would produce monovariant (one c -axis) or multi-variant (2 or 3 c -axes parallel to the $\langle 100 \rangle$ of the FCC disordered phase) particles depending on if there are one or more nuclei per particle, respectively.

Annealing of the nanoparticles causes the nanoparticles to lose their assembly as observed for a moderate anneal in Fig. 9. With further annealing the nanoparticles form into agglomerates (such as in Fig. 10) due to the loss of steric repulsion. The result is the formation of high-angle boundaries making another mechanism for ordering viable. This second mechanism is analogous to that reaction described for ordering and recrystallization. Because the agglomerates contain nanoparticles randomly oriented with respect to

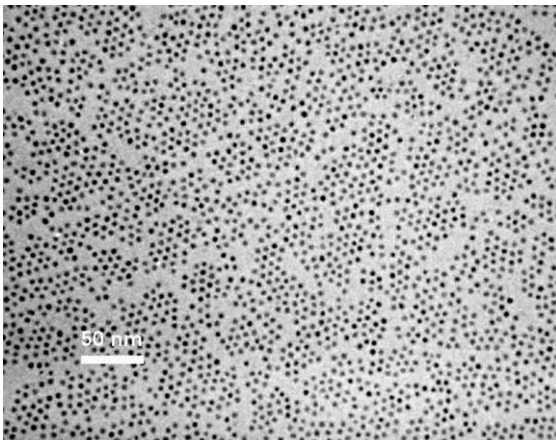


Fig. 9. Loss of assembly in FePt nanoparticles due to moderate annealing.

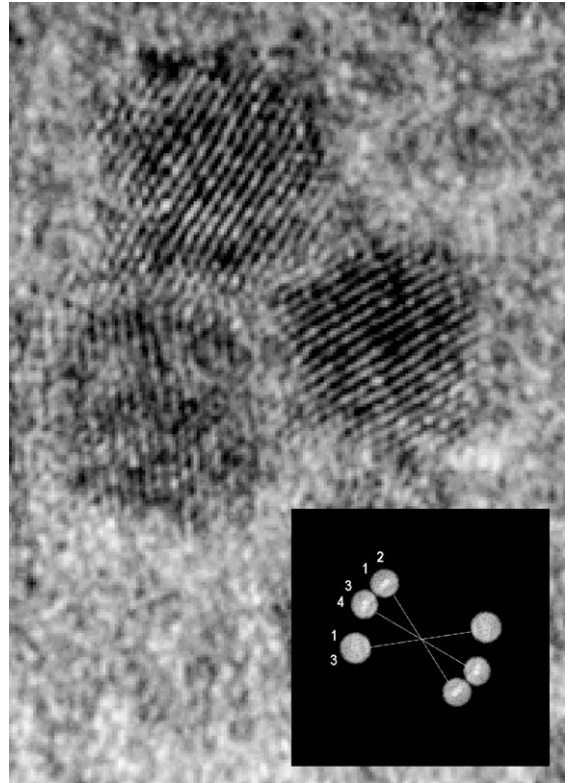


Fig. 10. Agglomeration of nanoparticles producing high-angle grain boundaries.

each other (as shown in Fig. 10), there exist incoherent high-angle grain boundaries, which can also act as nucleation sites for ordering and act as the ordering reaction front as well as decreasing the total surface energy via grain growth.

These two possibilities for ordering produces a solid-state transformation containing at the very least two competing reaction fronts whose number and velocity must be controlled for the ultimate production of magnetic recording media. Of course this simplistic view does not take into consideration finite size effects on the ordering process, which could be considerable. But the TTT curve for ordering and therefore the ordering kinetics will be intimately controlled by the microstructure of the as-deposited and the rearrangement of the defect structure. The incoherent high-angle boundary mechanism may provide for faster ordering kinetics. Additionally, sintering

mechanisms, which occur within agglomerates such as surface diffusion, vacancy diffusion and grain boundary diffusion may also substantially enhance the ordering kinetics. However, the resulting microstructure is not beneficial for magnetic recording and therefore must be avoided. The result is that the more beneficial mechanism for ordering (ordering of a lone nanoparticle) may actually require longer annealing times and/or higher temperatures.

8. Conclusions

It has been shown that the mechanisms for chemical ordering are strongly dependent on the defect structure that develops as a result of other solid-state reactions such as recrystallization. These observations have been formulated in a systematic way and further developed for solid-state reactions such as grain growth and sintering which have been observed in SOMA based on $L1_0$ FePt nanoparticles. Clearly for SOMA to reach its full potential as ultra-high-density magnetic recording media the avoidance of the sintering must be accomplished. In this article we have described a simplistic way of looking at these combined reactions and based on bulk reactions we have established several different possible mechanisms for ordering which may be occurring at the same time and give rise to the observed ordering kinetics. It is required that some of these mechanisms must be eliminated such that only the ordering mechanisms remain which keep the desired self-assembly of the pre-annealed state.

References

- [1] T. Klemmer, D. Hoydick, H. Okumura, et al., *Scr. Metall. Mater.* 33 (10–11) (1995) 1793.
- [2] D. Weller, A. Moser, *IEEE Trans. Magn.* 35 (6) (1999) 4423.
- [3] S. Sun, C.B. Murray, D. Weller, et al., *Science* 287 (2000) 1989.
- [4] Z.R. Dai, S. Sun, Z.L. Wang, *Nano Lett.* 1 (8) (2001) 443.
- [5] E. Hornbogen, *Metall. Trans. A* 10A (1979) 947.
- [6] D.A. Porter, K.E. Easterling, *Phase Transformations in Metals and Alloys*, Chapman & Hall, New York, 1981.
- [7] E.A. Guggenheim, *Mixtures*, Clarendon Press, Oxford, 1952.
- [8] L.D. Landau, L.E. Lifshitz, *Statistical Physics*, 3rd Edition, Pergamon Press, Oxford, 1980.
- [9] W.A. Soffa, D.E. Laughlin, *Acta Metall.* 37 (11) (1989) 3019.
- [10] G.M. Gushchin, F.N. Berseneva, *Phys. Met. Metall.* 15 (1987) 6.
- [11] B. Zhang, *Phase Transformation and Interrelationship between Microstructure, Domain Structure and Magnetic Properties in Polytwinned Fe-Pt and Fe-Pd Alloys*, Ph.D. Thesis, University of Pittsburgh, 1991.
- [12] N.A. Sokolovskaya, N.N. Shchegoleva, G.S. Kandaurova, *Fiz. Met. Metalloved.* 41 (1) (1976) 55; B. Zhang, M. Lelovic, W.A. Soffa, *Scr. Metall. Mater.* 25 (1991) 1577.
- [13] G. Hadjipanayis, P. Gaunt, *J. Appl. Phys.* 50 (3) (1979) 2358.
- [14] T.A. Dzigrashvili, M.V. Dzhibuti, V.V. Kokorin, et al., *Fiz. Met. Metalloved.* 43 (6) (1977) 1316; R. Oshima, M. Sugiyama, F.E. Fujita, *Metall. Trans. A* 19A (1988) 803; G.M. Gushchin, Ye.I. Teytel, V.S. Litvinov, *Phys. Met. Metall.* 69 (2) (1990) 156.
- [15] M. Hirabayashi, S. Weissmann, *Acta Metall.* 10 (1962) 25.
- [16] L. Chen, Y. Wang, A.G. Khachaturyan, *Philos. Mag. Lett.* 65 (1) (1992) 15.
- [17] B. Zhang, W.A. Soffa, *Phys. Status Solidi A* 131 (1992) 707.
- [18] R.A. Ristau, K. Barmak, K.R. Coffey, et al., *J. Mater. Res.* 14 (8) (1999) 3263.
- [19] A.Y. Yermakov, V.V. Maykov, *Phys. Met. Metall.* 60 (4) (1985) 113; B. Zhang, T. Klemmer, D. Hoydick, et al., *IEEE Trans. Magn.* 30 (2) (1994) 589.
- [20] H. Okumura, W.A. Soffa, T.J. Klemmer, et al., *IEEE Trans. Magn.* 34 (4) (1998) 1015.
- [21] T.J. Klemmer, *Ordering, Recrystallization and Microstructural Development in FePd Permanent Magnet Alloys*, Ph.D. Thesis, University of Pittsburgh, 1995.
- [22] F.J. Humphreys, M. Hatherly, *Recrystallization and Related Annealing Phenomena*, Elsevier, Tarrytown, NY, 1996.
- [23] T. Klemmer, W.A. Soffa, in: W.C. Johnson, D.E. Laughlin, W.A. Soffa (Eds.), *Solid-Solid Phase Transformations*, The Minerals, Metals and Materials Society, Warrendale, PA, 1994, p. 969.
- [24] C.M.F. Rae, in: C.S. Pande, D.A. Smith, H.A. King, et al. (Eds.), *Interface Migration and Control of Microstructure*, ASM, Detroit, MI, 1984, p. 145.